Engineering

Electrical Engineering fields

Okayama University *Year* 1997

The state-of-the-art of power electronics in Japan

Hirofumi Akagi
Okayama University

The State-of-the-Art of Power Electronics in Japan

Hirofumi Akagi, *Fellow, IEEE*

***Abstract*— Since the late 1950's, power electronics has been developing by leaps and bounds without saturation to become the key technology essential to modern society and human life as well as to electrical engineering. This paper mainly focuses on the state-of-the-art of power electronics technology and its medium to high-power applications because the author cannot survey the whole spectrum of power electronics ranging from a 5-W switching regulator to a 2.8-GW high-voltage dc transmission system now under construction in Japan. This paper also presents prospects and directions of power electronics in the 21st century, including the personal views and expectations of the author.**

***Index Terms*— AC motor drives, active filters, power converters, power devices, power electronics.**

I. Introduction

POWER electronics have been initiated by the invention and production of thyristors or silicon-controlled rectifiers. In conjunction with microcomputers and digital signal processors (DSP's) brought by microelectronics technology, the following great leaps have been made in power electronics technology and applications:

1) remarkable progress in the capacity and switching speed of gate-turn-off (GTO) thyristors and insulated gate bipolar transistors (IGBT's);
2) establishment in theory and practice of the so-called "vector-controlled ac motor drives" and their prevalence over and replacement of dc motor drives;
3) penetration into utility applications such as an 80-MVA inverter-based static var compensator using GTO thyristors, and a 300-MW high-voltage dc transmission system using light-triggered thyristors (LTT's).

Applications of power electronics are still expanding into industry and utility, so that the term "power electronics" in the 21st century will have a much broader meaning than it did in the 1980's. For instance, the marriage of power electronics and power engineering will bear flexible ac transmission systems in the near future, unless the two get a divorce. Generally, developments in power electronics yield needs of power electronics, so that the needs induce the developments in turn, as if to constitute a positive feedback system.

This paper presents the state-of-the-art of power electronics in Japan, along with its prospects and directions in the 21st century, including the personal views and expectations of the author. This paper is organized as follows. Section II describes the present status and future trends of power semiconductor devices in Japan. Section III presents static power converters, focusing on pulse-width-modulation (PWM) inverters, which are classified according to their applications. Section IV describes a 450-kHz 4-kW voltage-source series-resonant inverter and its specific application for dental casting machines. Section V shows the present status of the steel industry, which has already introduced large-capacity high-performance vector-controlled induction/synchronous motors into hot- and cold-strip-mill drives. Section VI is focused on vector-controlled induction motor drive systems with and without speed sensors. Sections VII–IX describe utility applications of power electronics: a 2.8-GW high-voltage direct-current (HVDC) transmission system, 300–400-MW adjustable-speed pumped-storage generator/motor systems controlled by line-commutated cycloconverters or PWM rectifier/inverters, and a 48-MVA active filter for power conditioning.

Manuscript received November 4, 1996; revised May 28, 1997. Recommended by Associate Editor, L. Xu.

The author is with the Department of Electrical Engineering, Okayama University, Okayama-City, 700 Japan (e-mail: akagi@power.elec.okayama-u.ac.jp).

Publisher Item Identifier S 0885-8993(98)01943-7.

II. Power Semiconductor Devices

Power semiconductor devices are indispensable to power electronic systems, like bread or rice is to the human system. No remarkable progress could be made in power electronic technology unless there were an emergence of new power devices or a significant improvement of already existing devices.

A. Light-Triggered Thyristors

LTT's rated at 8 kV and 3.5 kA (average current) have been developed with a forward voltage drop of 2.7 V at 3.5 kA [1]. The thyristors are fabricated on a silicon wafer with a 6-in diameter. The main reason for applying light-triggering technology to the thyristor is that light signals are not affected by electromagnetic interference (EMI). In addition, light is conducted through an optical glass fiber, which is one of the best insulation materials. This ensures sufficient insulation between a system controller operating at ground potential and a gate-drive circuit operating at potentials as high as, or exceeding, 250 kV [2].

B. Gate-Turn-Off Thyristors and Static Induction Thyristors

GTO thyristors rated at 6 kV and 6 kA, fabricated on a silicon wafer with a 6-in diameter, are now available to high-power inverters for utility/industry applications [3]. The GTO thyristors have the capability of shutting off an anode current of 6 kA with the help of a snubbing circuit, but the average anode current is designed to be about 2 kA in practical application. Extremely high-voltage GTO thyristors aimed at 9–12-kV ratings will be developed in the near future, using leading edge semiconductor technology.

Fig. 1. Rectangular press-pack reverse-conducting IGBT rated at 2.5 kV and 1 kA.

A static induction (SI) thyristor rated at 4 kV and 200 A (average current) has been developed, which has the capability of shutting off an anode current of 1 kA or more. The SI thyristor equipped with a snubbing capacitor of 0.1 μF can operate at 4 kHz, which is much higher than the switching frequency limitation of the same class of GTO thyristor [3]. However, the SI thyristor has not yet come on the market.

C. Insulated Gate Bipolar Transistors

Over the last ten years, a significant reduction in conducting and switching losses in IGBT's has been achieved in the process of transition from the first, via the second, to the third generation. At present, the third-generation IGBT's rated at 600, 1200, and 1700 V are widely used for general inverter applications with current ratings up to 600 A or more. They are packaged with soft-recovery free-wheeling diodes into power modules, so that they are often called "IGBT modules" in Japan. They have the advantage of not requiring any electric isolation from heat sinks, thus making inverters compact. Moreover, IGBT modules rated at 2000 V and 500 A are available and used mainly for electric traction.

The Fuji Electric Company has recently developed a rectangular press-pack reverse-conducting IGBT rated at 2.5 kV and 1 kA [4]. This IGBT has the following electric characteristics:

1) maximum turn-off collector current of 5 kA;
2) saturation voltage of 4.4 V at $I_C = 1$ kA and 125°C;
3) fall time of 0.85 μs;
4) rise time of 1.6 μs.

Fig. 1 is a photograph of the IGBT. The size of the rectangular press pack is $133^W \times 110^H \times 20^D$ (mm). Nine IGBT chips and three diode chips are integrated into the package, and the size of either the single IGBT or diode chip is a square of 20 $\times$ 20 (mm). This package structure efficiently removes heat from both top and bottom, so the IGBT is more suitable to electric traction applications requiring high reliability. The Fuji Electric Company has also developed a rectangular press-pack reverse-conducting IGBT rated at 1.2 kV and 2 kA for high-frequency resonant inverters. This IGBT has a very low forward voltage drop of 3.7 V at $I_C = 2$ kA and 125°C. Fig. 2 shows the turn-off waveforms of $v_{\rm CE}$ and i_C in hard-switching operation under the conditions of $V_{\rm DC} = 600$ V, $I_C = 2$ kA, and $T_j = 25$°C in (a) and $T_j = 125$°C in (b). These IGBT's in a rectangular press pack are now available on the market.

Hitachi has developed a 3.5-kV 500-A IGBT module with a forward voltage drop of 5.6 V at $I_C = 325$ A [5]. According to [3], 4.5 kV would be a final goal for IGBT's to reach, and therefore such a high-voltage IGBT is expected to take the place of 4.5-kV GTO thyristors in the near future.

To advance performance beyond the third-generation IGBT's, the fourth-generation devices will require exploiting fine-line lithographic technology and/or employing the trench technology currently being used to produce a new power MOSFET with very low on-state resistance. The fourth-generation IGBT will have a forward voltage drop as low as 1.5 V for a 600-V device or 2.0 V for a 1200-V device at each rated current.

An intelligent IGBT or an intelligent power module (IPM) is available which is an attractive power device integrated with circuits to protect against overcurrent, overvoltage, and/or overheat. This intelligent IGBT based on the fourth generation will take a few years to come on the market.

III. Static Power Converters

The development of static power converters depends strongly on both power semiconductor devices and utility/industry needs.

A. High-Power Inverters

Table I summarizes future trends of high-power converters with the focus on their capacity in 1996, 2001, and 2006. It is impossible to find any application of phase-controlled thyristor converters and cycloconverters, except for high-voltage dc transmission systems and extremely large-capacity synchronous motor drive systems. A voltage-source inverter

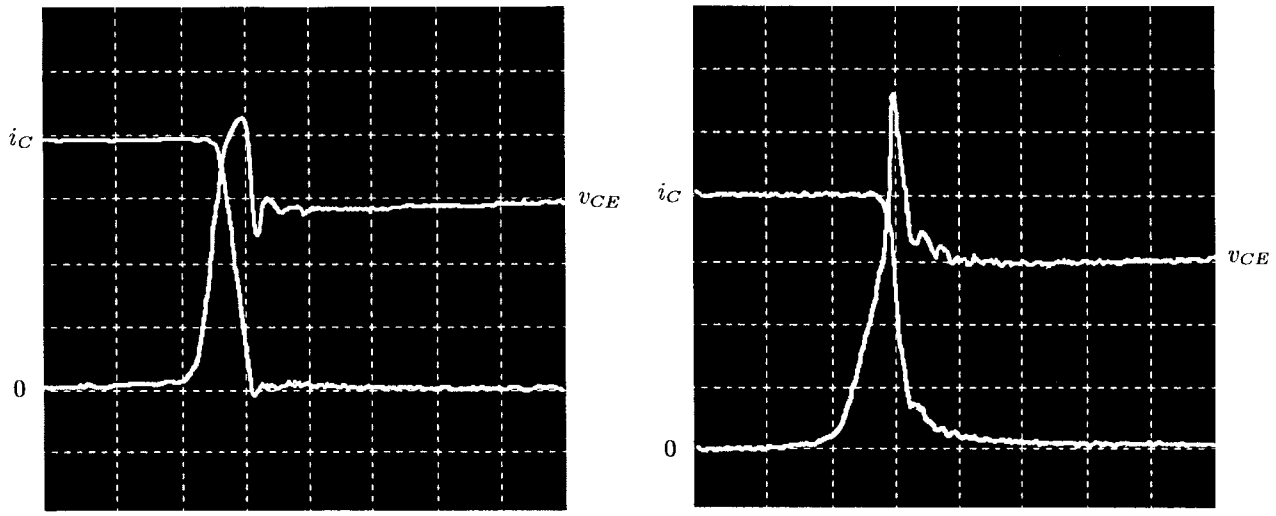

Fig. 2. Turn-off waveforms of the rectangular press-pack reverse-conducting IGBT rated at 1.2 kV and 2 kA (200 V/div, 500 A/div, and 200 ns/div): (a) $T_j = 25°C$ and (b) $T_j = 125°C$.

TABLE I
FUTURE TRENDS IN CAPACITY OF HIGH-POWER CONVERTERS

Year	1996	2001	2006
LTT	300 MVA	1000 MVA	3 GVA
GTO	80 MVA	300 MVA	1000 MVA
IGBT	2 MVA	5 MVA	20 MVA

using GTO thyristors in a range of 200–300 MW is due to be put into practical use by 2001 [6]. Its "back-to-back" connection is intended for providing asynchronous ac linkage between two power systems with flexibility. This high-power inverter would also be essential to unified power flow controllers in the Flexible AC Transmission System (FACTS) concept initiated in the United States.

Figs. 3–6 show possible circuit configurations of high-power inverters using twelve GTO thyristors for steel-mill drives and utility applications. Fig. 3 is referred to as a neutral-point-clamped voltage-source inverter or a three-level voltage-source inverter [7]. Figs. 3–5 are suitable for ac motor drives because no transformer is connected to the ac terminals of the inverters. Mitsubishi has developed a three-phase 10-MVA three-level PWM rectifier/inverter consisting of 24 GTO thyristors rated at 6 kV and 6 kA in which the dc-link voltage is 6 kV [8]. This rectifier/inverter feeds a 6-MW synchronous motor for steel-mill drives. Toshiba has developed a three-phase 1.2-kV, 1.8-MVA three-level PWM inverter using IGBT modules rated at 1.7 kV and 400 A for vector-controlled induction motor drives, with or without a speed sensor, in industrial plants [9]. However, multilevel inverters, such as four- or five-level inverters, have not yet been practically applied, although they are being researched in universities and institutes. Fig. 5 shows multiconnection by means of separating and isolating three stator windings from the neutral point of an ac motor. It would be possible for the three-level

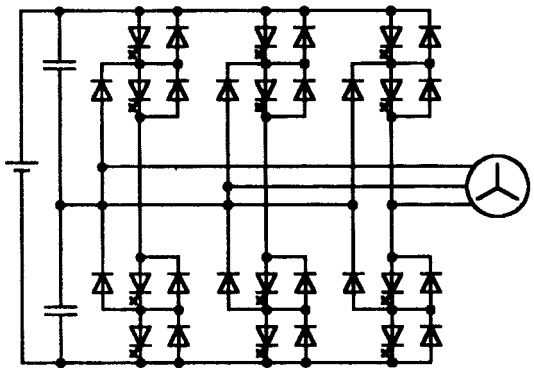

Fig. 3. Neutral-point-clamped (three-level) inverter.

inverter shown in Fig. 3 to take the place of the two-level inverters shown in Figs. 4 and 5.

Fig. 6 shows the multiconnection of a couple of two-level inverters by means of two three-phase transformers, the primary windings of which are connected in series. It is also possible to combine Fig. 3 with Fig. 6, thus resulting in higher power and less harmonics. Fig. 6 and the combination of Fig. 6 with Fig. 3 are effective in utility applications such as static var compensators. However, practical technology capable of achieving series connection of more than thirty GTO thyristors is required for high-voltage dc transmission systems.

B. Applications for Rolling Stock

Since March of 1992, new high-speed trains referred to as Nozomi[1] or the third-generation Shinkansen have been in commercial service with a maximum speed of 270 km/h. The power electronic circuit for electric traction consists of two-level voltage-source PWM rectifier/inverters using GTO thyristors rated at 4.5 kV and 2.5 kA. The high-speed train, consisting of 16 cars with a nominal seating capacity of 1323

[1] Nozomi in Japanese means "hope" in English.

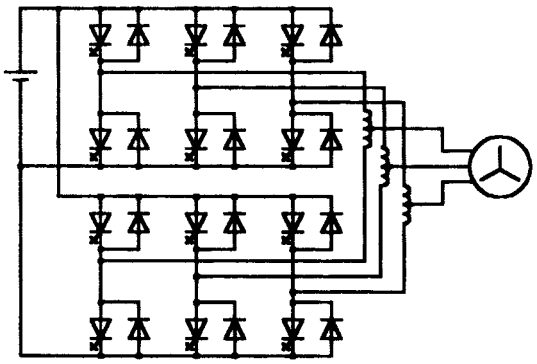

Fig. 4. Multiconnection using interphase transformers.

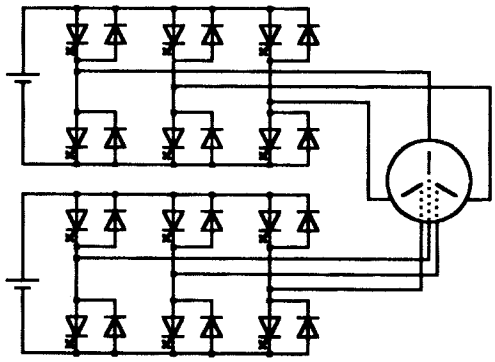

Fig. 5. Multiconnection by means of isolation.

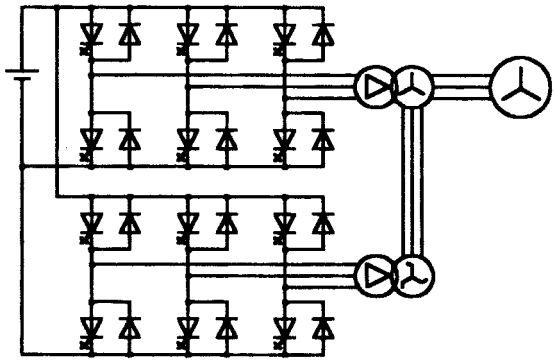

Fig. 6. Multiconnection using transformers.

is driven by 40 induction motors, each of which is rated at 300 kW, and therefore the maximum output power is 12 MW $(=300\ \text{kW} \times 40)$. For the next-generation three-level PWM rectifier/inverters using the 2.5-kV 1-kA press-pack IGBT's with a switching frequency of around 2 kHz are being developed by the Fuji Electric Company. These aim to replace the present GTO thyristor-based rectifier/inverters in the near future.

Newly developed 1.5-kV dc commuter trains are characterized by three-level PWM inverters using IGBT modules rated at 2 kV and 325 A. The unit capacity of each inverter is 375 kVA. This success has led to the proliferation of IGBT inverters for electric traction, accompanied by lower torque ripple, lower acoustic noise, and higher efficiency as well as smaller volume and lighter weight than GTO inverters.

C. General-Purpose Inverters

Over the last ten years, the emergence and advancement of IGBT modules have made voltage-source PWM inverters much more prevalent in general-purpose applications such as adjustable-speed ac motor drives, uninterruptible power supplies, and so on. At present, IGBT modules are taking the place of bipolar junction transistors (BJT's) because of their high-speed switching characteristics, simple drive circuits, and easy and compact power circuits. For example, voltage-source PWM rectifier/inverter systems using IGBT modules have been used as the power circuit for uninterruptible power supplies in the range of 10 kVA to 1 MVA. However, high-speed switching of IGBT modules might cause the following problems to which little attention has been paid:

1) conducted and/or radiated EMI;
2) ground current flowing through the stray capacitances between motor windings and frames;
3) bearing current and shaft voltage inside motors.

A soft-switched inverter such as the so-called "resonant dc-link inverter" [10] is a candidate for overcoming the above-mentioned problems, rather than for improving conversion efficiency. The resonant dc-link inverter, however, has not yet been put into practical use in Japan.

IV. High-Frequency Resonant Inverters

With significant progress in the development of IGBT's, MOSFET's and SI transistors (SIT's), high-power resonant inverters in a frequency range of 20 kHz to 2 MHz have been, or are being, put into practical use for induction heating and corona discharge treatment processes. There are two types of circuit configurations in the resonant inverters based on zero-voltage-switching (ZVS) and/or zero-current-switching (ZCS) techniques:

1) current-source parallel-resonant inverters;
2) voltage-source series-resonant inverters.

For instance, 200-kHz 200-kW current-source parallel-resonant inverters using SIT's have been employed for surface quenching in the automobile industry, and 350-kHz 600-kW voltage-source series-resonant inverters using MOSFET's are now available for tube welding [11]. A 2-MHz 10-kW voltage-source series-resonant inverter using MOSFET's is under development for low-temperature plasma heating. Moreover, 20–50-kHz 1–40-kW voltage-source series-resonant inverters using IGBT's have been integrated into corona discharge treaters for film. As an example, this section describes a 450-kHz 4-kW induction melting system for a dental casting machine [12].

A. System Configuration

Fig. 7 shows the system configuration consisting of a single-phase H-bridge voltage-source inverter using four MOSFET's rated at 450 V and 50 A, a step-down transformer with a turn ratio of 8:1, and a series-resonant circuit. Table II summarizes the rating and characteristics of the MOSFET (Hitachi 2SK1521). A lossless snubbing capacitor of 2000 pF is connected between the drain and source of each MOSFET

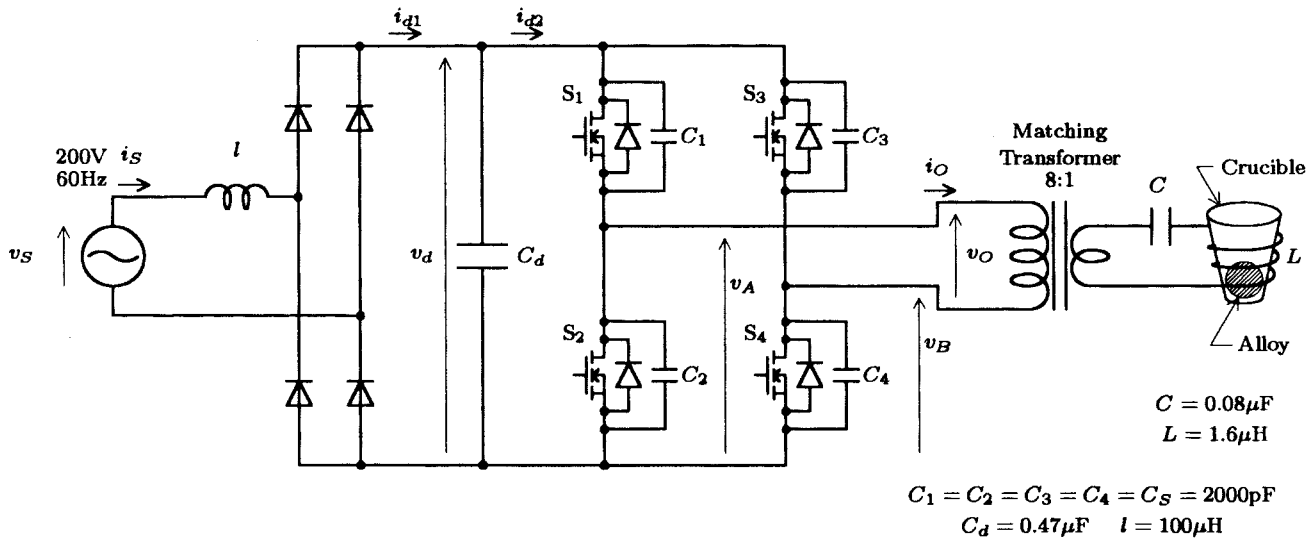

Fig. 7. System configuration of the voltage-source series-resonant inverter for induction melting.

TABLE II
RATING AND CHARACTERISTICS OF MOSFET (2SK1521)

drain to source voltage	450 V
drain current	50 A
on-state resistance	0.08 Ω
input capacitance	8700 pF
output capacitance	2400 pF
turn-on delay time	85 ns
rise time	250 ns
turn-off delay time	600 ns
fall time	250 ns

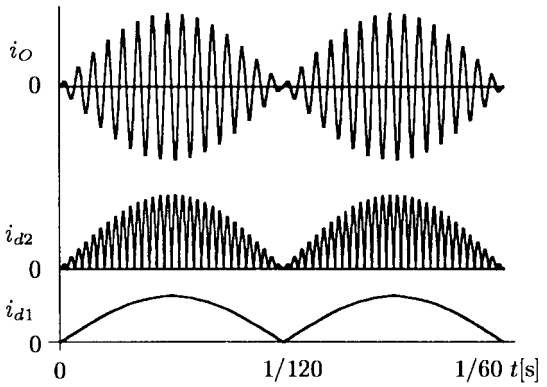

Fig. 8. Current waveforms under assumption that the operating frequency is 1.8 kHz and the line frequency is 60 Hz.

to achieve ZVS. Several grams of an alloy of Cr–Co–Mo in a crucible are required to melt within about 30 s in order to prevent it from oxidizing in the dental casting machine. The dc power supply for the inverter is a single-phase diode-bridge rectifier containing neither a dc smoothing electrolytic capacitor nor a reactor except for a high-frequency capacitor of 0.47 μF. Thus the dc voltage across the high-frequency capacitor is fluctuating at 120 Hz, that is, twice as high as the line frequency of 60 Hz.

Fig. 8 shows the current waveforms of i_O, i_{d1}, and i_{d2} under the assumption that the operating frequency is 1.8 kHz and the line frequency is 60 Hz, making the waveforms clear. The envelopes of i_O and i_{d2} fluctuate at twice the line frequency because of no dc smoothing capacitor. Note that i_{d1} becomes a ripple-free waveform which is proportional to the dc-link voltage because the high-frequency capacitor absorbs the high-frequency current ripple included in i_{d2}. This inverter plus the series-resonant circuit looks like a pure resistor when it is seen from the dc terminals of the rectifier. Thus, the line current of the rectifier becomes a sinusoidal waveform with unity power factor as long as the line voltage is sinusoidal. The fluctuation of the output power at twice the line frequency produces no effect on the induction melting process.

B. Experimental Waveforms

Figs. 9 and 10 show the experimental waveforms of the 450-kHz 4-kW induction melting system. The quality factor of the series-resonant circuit for the dental casting machine is about 30. The time constant of the envelope of the resonant current is given by

$$\tau = 2Q/\omega_r = 2 \times 30/(2\pi \times 450 \times 10^3) = 21\ \mu\text{s}.$$

The output power control based on pulse-density modulation (PDM) enables ZCS in all the operating conditions. Fig. 9 shows the waveforms of the inverter output voltage and current in the case of full power operation of about 3.6 kW.

Because the 2000-pF snubbing capacitor suppresses dv/dt, that is, the derivative of the drain to source voltage with respect to time, the voltage rise-time is about 150 ns. Note that no voltage spike occurs in the output voltage. Fig. 10 corresponds to the case of operation at a pulse density of 12/16. The amplitude of i_O in Fig. 10 becomes smaller than that in Fig. 9. Aside from the PDM control, no decay appears in the amplitude of i_O in Fig. 10 because τ is longer than the PDM period of $T = 9\ \mu$s. The inverter properly operates at a

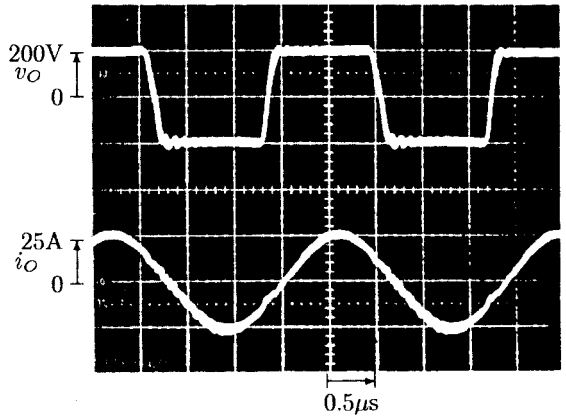

Fig. 9. Output voltage and current waveforms of the inverter operating at unity pulse density.

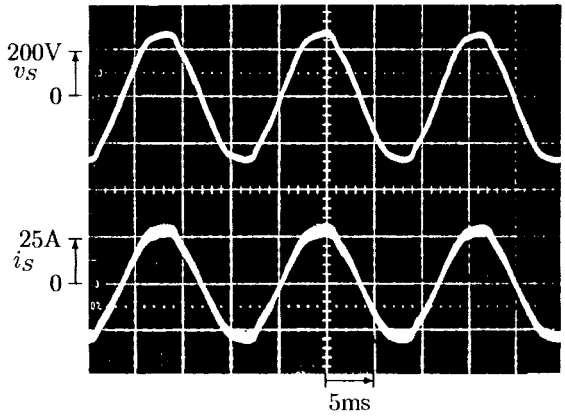

Fig. 11. Input voltage and current waveforms of the diode rectifier under unity pulse density.

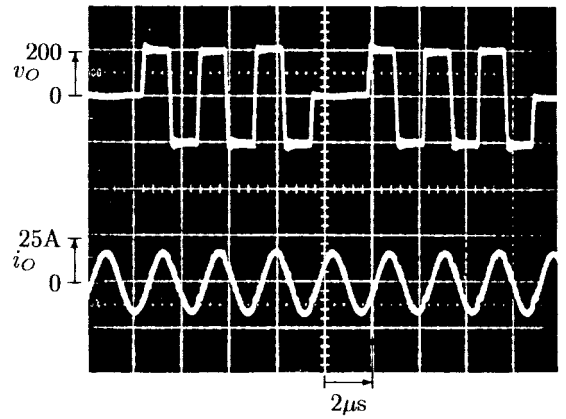

Fig. 10. Output voltage and current waveforms of the inverter operating at pulse density 12/16.

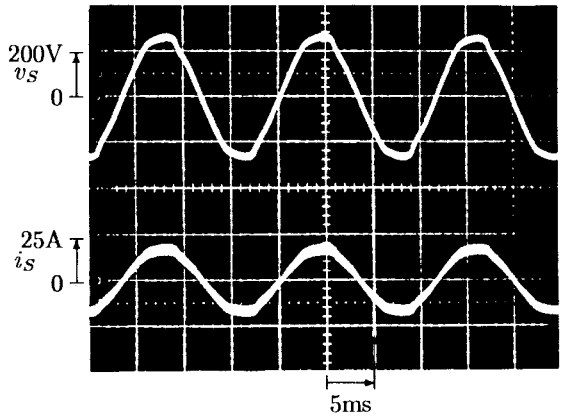

Fig. 12. Input voltage and current waveforms of the diode rectifier under pulse density of 12/16.

pulse density as low as 2/16. In this case, the output power is reduced to 80 W, that is, only 2.2% of 3.6 kW.

Figs. 11 and 12 show the waveforms of the line voltage and current of the diode rectifier. Fig. 11 corresponds to the case of full power operation at unity pulse density, and Fig. 12 corresponds to the case of operation at a pulse density of 12/16. The line current is an almost sinusoidal waveform with unity power factor, the amplitude of which depends on the pulse density.

The voltage-source series-resonant PDM inverters are capable of adjusting the output power by themselves, as well as of performing both ZVS and ZCS in all the operating conditions. Hence, they have been practically applied in dental casting machines of 200–450 kHz, 2–5 kW, and corona discharge treaters of 20–50 kHz and 1–40 kW.

V. Steel-Mill Drives

The steel industry in Japan has been actively introducing new technologies of power electronics and motor drives since the beginning of the 1960's. Table III summarizes the present status of steel-mill drives in Japan. Hot-strip-mill drives require larger motors than cold-strip-mill drives, whereas cold-strip-mill drives require higher control performance than hot-strip-mill drives [13]. The reason for applying line-commutated cycloconverters operating with *circulating current* mode at the expense of a lower power factor in hot-strip-mill drives rated at more than 5 MW is that the cycloconverter output frequency required in hot-strip-mill drives ranges up to around 40 Hz, which is too high for line-commutated cycloconverters having an input (line) frequency of 50/60 Hz to operate in *circulating current-free* mode. Replacement of conventional electrically triggered thyristors with LTT's makes the cycloconverters more reliable and compact.

With the continuous increase in the voltage/current ratings of GTO thyristors, PWM rectifier/inverters using GTO thyristors tend to be preferred to line-commutated cycloconverters because they have the capability of operating at unity power factor with less harmonics on the line side. However, PWM rectifier/inverters are at present inferior in efficiency to cycloconverters. We have to think out a viable and cost-effective solution to reduce snubbing losses in the PWM rectifier/inverter [8].

VI. Vector-Controlled Induction Motor Drives

A. Vector Control with Speed Sensor

Vector-controlled induction motors with shaft encoders or speed sensors have been widely applied in combination with

TABLE III
VECTOR-CONTROLLED AC MOTOR DRIVE SYSTEMS FOR STEEL MILLS

	Cold-Strip Mill	Hot-Strip Mill
Capacity	below 5 MW	over 5 MW
Motor	squirrel-cage induction motor	synchronous motor
Control	vector control with shaft encoder	vector control with shaft encoder
Power Circuit Configuration	voltage-source PWM rectifier/inverter (two-level or three-level)	12-pulse line-commutated cycloconverter operating with circulating current mode
Overall Efficiency	91% (at 5 MW)	93% (at 5 MW)
Issues	snubbing loss, less compact	poor power factor, harmonics

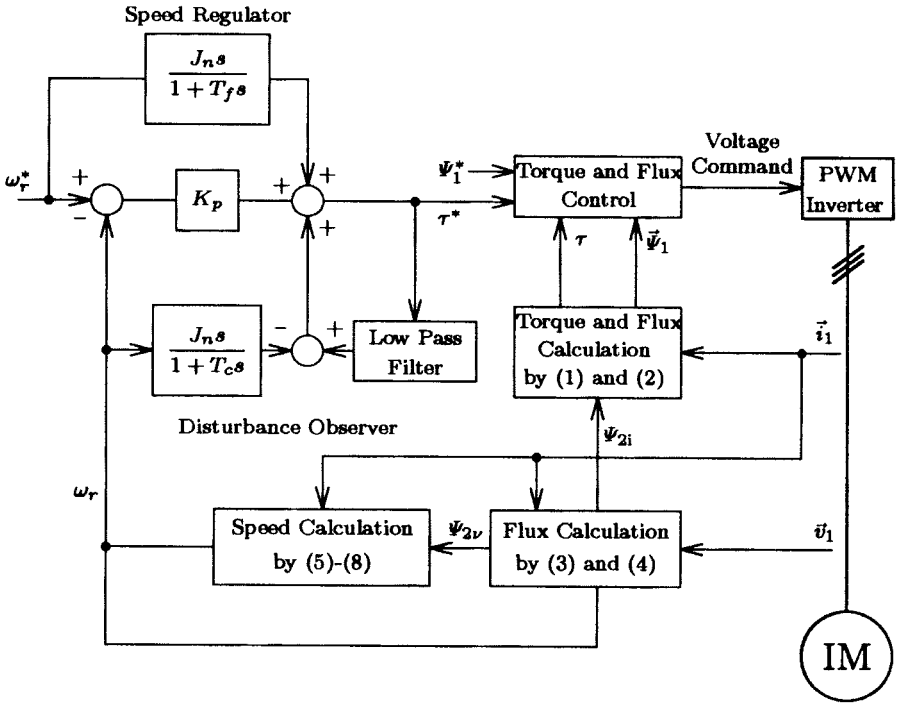

Fig. 13. System block diagram of the sensorless drive characterized by a speed-control range of 1:75.

voltage-source PWM inverters using IGBT modules. According to the specification of new products sold by the Toyo Electric Company, vector-controlled induction motor drive systems ranging from 1.1 kW to 1 MW provide the following performance specifications:

1) a broad range of speed control (1:1000) with speed-control accuracy of $\pm 0.01\%$;
2) constant torque operation in a speed range of 1.8–1800 rpm;
3) high torque starting at 150% of the rated torque.

B. Vector Control Without Speed Sensor

Recently, many researchers and engineers have made a significant effort toward improving the performance of speed-sensorless vector-controlled induction motor drive systems. As a result of keen competition among Japanese companies such as Hitachi, Toshiba, Mitsubishi, Fuji, Meiden, Yaskawa, and so on, various kinds of control systems have been proposed and implemented with voltage-fed PWM inverters [14], [15]. A good market is developing for the speed-sensorless systems as the price gradually decreases due to device cost reduction and power electronics integration strategies.

Miyashita *et al.* have developed speed-sensorless vector-controlled induction motor drive systems characterized by a wide range of speed control, which are now available from the Toyo Electric Company [16]. Fig. 13 shows the system block diagram of the sensorless drive based on the space vector theory, which is different in principle from a conventional system oriented to the secondary interlinkage flux vector. Speed-sensorless vector-controlled induction motor drive systems ranging from 1.1 kW to 1 MW provide the following good performance:

1) a wide range of speed control (1:75) with speed-control accuracy of $\pm 0.5\%$ and speed response of 90 rad/s;
2) constant torque operation in a speed range of 24 rpm to 1800 rpm with torque accuracy of $\pm 3\%$ and torque response of 1000 rad/s;
3) high-torque starting at 150% of the rated torque.

1) Flux Estimation: The stator interlinkage flux vector $\vec{\Psi}_1$ and the instantaneous motor torque τ are calculated by (1)

and (2)

$$\vec{\Psi}_1 = L_\sigma \vec{i}_1 + \vec{\Psi}_{2i} \tag{1}$$

$$\tau = |\vec{\Psi}_1 \times \vec{i}_1| = |\vec{\Psi}_{2i} \times \vec{i}_1| \tag{2}$$

$$L_\sigma = L_1 - \frac{M^2}{L_2}.$$

Here, $\vec{\Psi}_{2i}$ is given by

$$\vec{\Psi}_{2i} = \int \left(\frac{M}{L_2} R_2 \vec{i}_1 - \frac{R_2}{L_2} \vec{\Psi}_{2i} + j\omega_r \vec{\Psi}_{2i} \right) dt. \tag{3}$$

In the above equations, L_1, L_2, and M are the primary inductance, secondary inductance, and mutual inductance, respectively, on a per-phase base in the T-type equivalent circuit. Note that another rotor interlinkage flux vector defined by (3) is called the "current model flux vector" $\vec{\Psi}_{2i}$. The reason for applying the current model flux Ψ_{2i} into the torque control loop is that the current model flux is superior in stability to the so-called "voltage model flux," especially in the low-speed region. However, the calculation of the current model flux includes the motor speed ω_r, as shown in (3).

The estimated torque τ from (2) is compared to its reference torque τ^*. The error signal between them controls the voltage component of a voltage-source PWM inverter driving an induction motor. In an actual system, the rotor flux interlinkage vector $\vec{\Psi}_2$ is calculated by the following:

$$\vec{\Psi}_2 = \frac{L_2}{M} \int (\vec{v}_1 - R_1 \vec{i}_1 - pL_\sigma \vec{i}_1)\, dt + K \int (\vec{\Psi}_{2i} - \vec{\Psi}_2)\, dt. \tag{4}$$

The first term on the right-hand side of (4) is called the "voltage model flux vector." It is superior in transient response to the current model flux vector, whereas it is inferior in stability to the current model flux vector. The second term based on the current model flux plays an important role in suppressing a drift incurred by the integration of voltage and current in the first term, thus making a significant contribution to improving instability in the steady state of the low-speed region. In other words, the second term works to decrease the error between $\vec{\Psi}_2$ and $\vec{\Psi}_{2i}$ in the steady state.

2) Speed Estimation: Differentiating the phase angle of $\vec{\Psi}_2$ with respect to time on the stationary reference frame produces its angular frequency, that is, the rotating angular speed of the rotor flux interlinkage ω_2. The slip frequency ω_s is calculated from detected voltages and currents, as discussed later. As a result, the rotor speed ω_r can be estimated as follows:

$$\omega_r = \omega_2 - \omega_s. \tag{5}$$

In order to estimate the slip frequency ω_s, two frequencies, ω_{s1} and ω_{s2}, are calculated as follows:

$$\omega_{s1} = \frac{R_2 |\vec{\Psi}_2 \times \vec{i}_1|}{|\vec{\Psi}_{2i}|^2} \tag{6}$$

$$\omega_{s2} = \frac{L_2 R_2 |\vec{\Psi}_2 \times \vec{i}_1|}{M^2 \vec{\Psi}_2 \cdot \vec{i}_1} \tag{7}$$

$$\omega_s = \omega_{s1} + K_s \int (\omega_{s2} - \omega_s)\, dt. \tag{8}$$

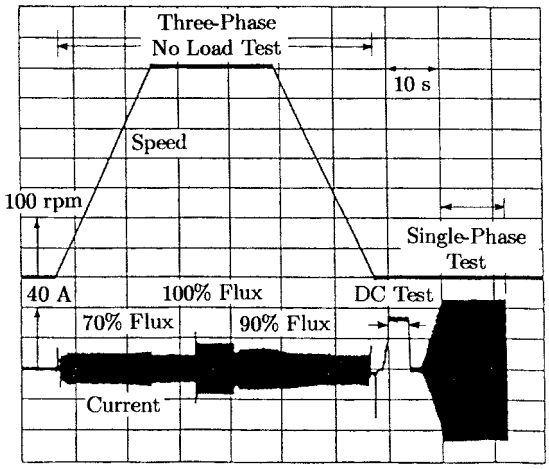

Fig. 14. Oscillograms of motor speed and current during automeasuring.

These are different in denominator from each other. The values calculated from (6) and (7) are theoretically the same in steady state. However, the value calculated from (6) may contain an error due to a variation in R_1, whereas that from (7) is not affected by the variation in R_1 because the denominator of (7) is the inner product of the two vectors $\vec{\Psi}_2$ and $\vec{i}_1$, where a vector concerning the variation in R_1 is perpendicular to the vector $\vec{i}_1$. However, the calculation of the denominator of (7) practically produces some error in transient states. The second term on the right-hand side of (8), therefore, is aimed at correcting the first term in the steady state.

3) Automeasuring of Parameters: Any speed-sensorless vector-controlled system requires information on motor parameters to realize high performance. Ohmori *et al.* have presented a speed-sensorless vector-controlled inverter equipped with automeasuring of the motor parameters [17]. Fig. 14 shows an oscillogram of motor speed and current during the automeasuring process. Automeasuring based on the T-type equivalent circuit of an induction motor is composed of the following three tests:

1) no-load test—measure the mutual inductance M and the iron loss conductance g_0;
2) dc test—measure the primary resistance R_1;
3) single-phase test—measure the leakage inductance l_1 and the secondary resistance R_2.

4) Applications: Speed-sensorless vector-controlled systems are mainly being applied to industrial motor drives in which it is difficult to attach speed sensors mechanically, for instance, newspaper printing machines. In addition, the replacement of dc motor drives with speed-sensorless induction motor drives results in higher reliability, maintenance-free operation, and lower costs coming from removing speed sensors or shaft encoders. Typical examples of application are discussed below.

Offset printing machines do not require high accuracy of speed control in normal operating conditions, but require a high response of starting and smooth rotation speeds as low as 1/70–1/100 of the rated speed during the plate cylinder cleaning operation and the setting of the form plate. In a conventional drive system, two motors are used; one is aimed

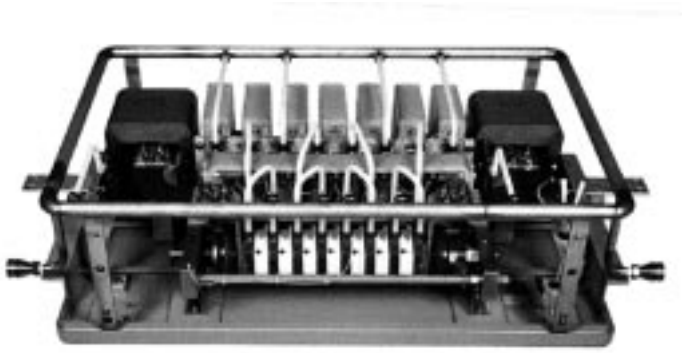

Fig. 15. Thyristor module consisting of seven LTT's rated at 6 kV and 2.5 kA.

at normal operation, and the other is exclusive for low-speed operation. A speed-sensorless vector-controlled system makes a single induction motor capable of achieving a wide range of speed control, thus replacing the two-motor system with a single motor.

As a replacement for dc motor drives, sensorless drive systems are now being applied to the helper roller in paper coating machines which do not require such high accuracy of speed control. The main roller, however, is still driven by a vector-controlled system with a speed sensor because the speed accuracy of today's sensorless vector-controlled systems is not sufficient for the main roller speed control.

VII. HVDC Transmission Systems

In 1993, an HVDC transmission system rated at 300 MW (250 kV and 1.2 kA) was installed in commercial service to supply a submarine cable transmission system under the channel between the islands of Hokkaido and Honshu. Each high-voltage thyristor valve in this system consists of a series connection of several thyristor modules. Fig. 15 is a photograph of a thyristor module consisting of a series connection of seven LTT's rated at 6 kV and 2.5 kA. The introduction of the LTT's makes a great contribution to the development of compact and reliable thyristor valves. Fig. 16 shows a thyristor valve used in this HVDC transmission system [18].

An HVDC transmission system of 1.4 GW (±250 kV and 2.8 kA) at the first stage and then 2.8 GW (±500 kV and 2.8 kA) at the final stage is now under construction, aimed at commercial operation by the beginning of the 21st century [1]. Fig. 17 and Table IV show the main circuit and specifications of the HVDC system using LTT's of 8 kV and 3.5 kA. The HVDC system will be able to control a bidirectional power flow of 2.8 GW through a 51-km-long submarine transmission cable and a 51-km-long overhead transmission line between the islands of Shikoku and Honshu. The main reason for introducing the HVDC system into such a short-distance power transmission system is that the 51-km-long submarine cable would impose restrictions on the sending power capacity in an HVAC system because a large amount of leading current would flow through nonnegligible parasitic capacitors in the submarine cable. Thus, the HVDC system is estimated to be lower in total construction costs than the HVAC system. The commercial operation of the HVDC system will result in achieving fast and precise power flow control irrespective of the difference between phase angles at the sending and receiving ac terminals, providing a higher degree of power stability in both power systems.

Fig. 16. Thyristor valves for the 250-kV 300-MW HVDC transmission system.

TABLE IV
Specifications of the HVDC System

First Stage Rating	1.4 GW ±250 kV
Second Stage Rating	2.8 GW ±500 kV
Overload Capacity	125% (3.5 kA)
AC Power System	500 kV 60 Hz

VIII. Adjustable-Speed Pumped-Storage Generator/Motor Systems

Recent progress in power electronic technology has made it possible to achieve adjustable-speed operation of 300–400-MW generators in hydroelectric power plants.

A. Line-Commutated Cycloconverter-Based System

In December 1993, a 400-MW adjustable-speed pumped-storage system was commissioned along with a 400-MW conventional constant-speed pumped-storage system at Ohkawachi hydroelectric power plant, owned and operated by the Kansai Electric Power Company of Japan [19], [20]. Fig. 18 shows the arrangement of the adjustable-speed pumped-storage system. The field windings of the 20-pole generator/motor of 400 MW are excited with three-phase low-frequency ac currents, which are supplied via slip rings by

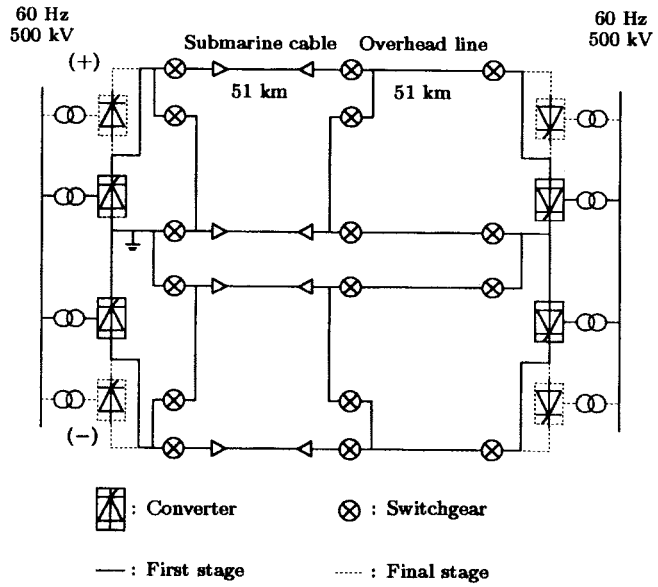

Fig. 17. Circuit configuration of the ±500-kV 2.8-GW HVDC transmission system.

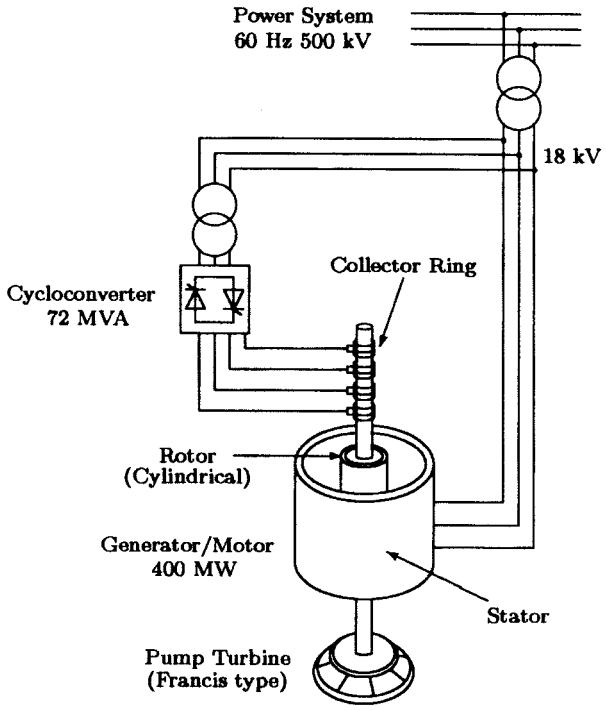

Fig. 18. Adjustable-speed pumped-storage system.

a 72-MVA 3-phase 12-pulse line-commutated cycloconverter. The armature terminals, rated at 18 kV, are connected to a 500-kV utility grid through a step-up transformer. The output frequency of the cycloconverter is controlled within ±5 Hz, and the line frequency is 60 Hz. This enables the cycloconverter to operate with *circulating current-free* mode in the adjustable-speed system, which has a synchronous speed of 360 rpm with a speed range from −8.3% (330 rpm) to +8.3% (390 rpm). Speed control provides the capability to control the input power in a range of ±80 MW in pump mode. This system was manufactured by Hitachi.

The 400-MW adjustable-speed pumped-storage generator/motor system has the following potential advantages over the conventional constant-speed system.

1) High-speed active power control can be achieved by the combination of the cycloconverter and the inertia effect of rotating parts. For instance, the actual input active power follows its reference with the ramp response spending 20 s from 256 to 400 MW in pump mode without any time delay. This makes a significant contribution to the improvement of frequency control, especially in pump mode at night.
2) The total operational efficiency of the system increases by 3%.
3) The stability of the adjustable-speed system under line fault and reclosing conditions is far superior to the conventional constant-speed system.
4) The adjustable-speed generator/motor system can be used as a FACTS device.

These excellent characteristics have been verified by field trials and subsequent commercial operation.

B. GTO Rectifier/Inverter-Based System

Another adjustable-speed system of 300 MW has been installed at the Okukuyotu II power plant owned and operated by the Electric Power Development Co., Ltd. A voltage-source PWM rectifier/inverter using GTO thyristors rated at 4.5 kV and 3 kA is connected between the stator and rotor winding terminals of the generator/motor instead of a line-commutated cycloconverter. The capacity of the GTO rectifier/inverter system is 40 MVA. The power circuit of each three-phase GTO rectifier is composed of three single-phase voltage-source PWM rectifiers, and six GTO rectifiers are connected to two excitation transformers, thus forming the GTO rectifier system having positive and negative dc terminals and a neutral terminal. The power circuit of each three-phase GTO inverter is a three-level voltage-source PWM inverter, and three GTO inverters are connected in parallel through ac reactors. This forms the GTO inverter system, the ac terminals of which are connected to the rotor terminals via three slip rings without transformers. The switching frequency of the GTO thyristors is 500 Hz [21]. This adjustable-speed system manufactured by Toshiba was commissioned last year.

IX. Active Filters for Power Conditioning

Attention has been paid to active filters for power conditioning: reactive power/negative-sequence compensation, harmonic compensation, harmonic damping, flicker compensation, and/or voltage regulation. Active filters in a range from 10 kVA to 60 MVA have been installed in Japan [22].

Fig. 19 shows a power system delivering electric power to the Japanese “bullet” trains on the Tokaido Shinkansen. Three shunt-active filters for compensation of fluctuating reactive current/negative-sequence current have been installed in the Shintakatsuki substation by the Central Japan Railway Company [23]. The shunt-active filters, manufactured by Toshiba, consist of voltage-fed PWM inverters using GTO thyristors, each of which is rated at 16 MVA. A high-speed train with a

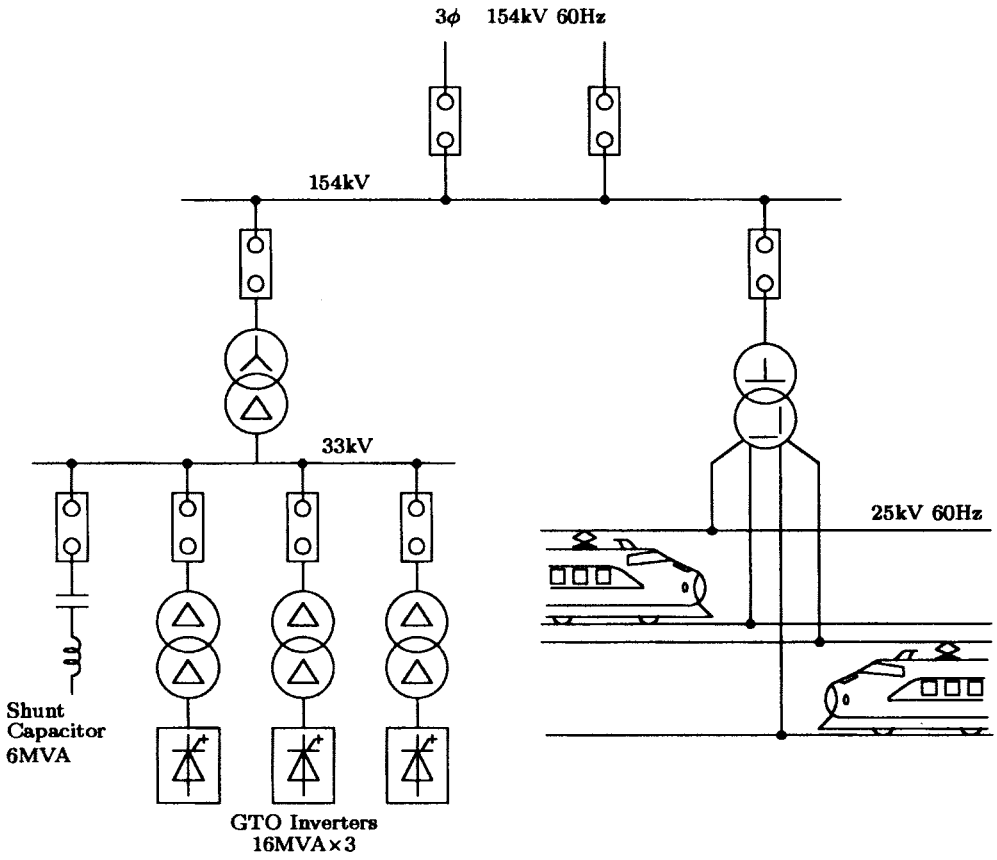

Fig. 19. The 48-MVA active filter installed for power conditioning in the Shintakatsuki substation.

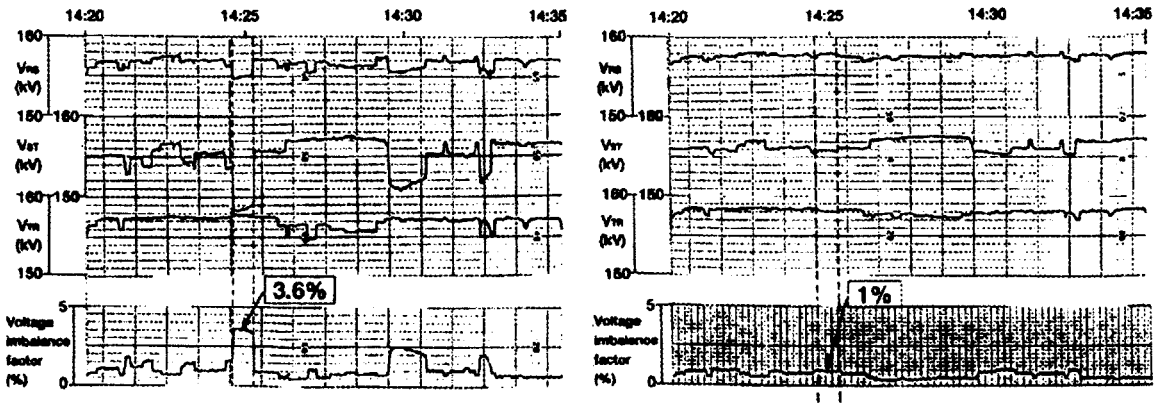

(a) (b)

Fig. 20. Compensation effect on the impact drop, variation, and imbalance of voltage: (a) before and (b) after compensation.

maximum output power of 12 MW draws unbalanced varying active and reactive powers from the Scott transformer, the primary of which is connected to the 154-kV utility grid. More than 20 high-speed trains pass per hour during the daytime. This causes voltage impact drop, variation, and imbalance at the terminals of the 154-kV utility system, accompanied by a serious deterioration in the power quality of other consumers connected to the same power system. The purpose of the shunt-active filters with a total rating of 48 MVA is to compensate for voltage impact drop, voltage variation, and imbalance at the terminals of the 154-kV power system and to improve the power quality. The concept of the instantaneous active and reactive power theory, or the so-called "*p-q* theory" [24] in the time domain, has been applied to the control strategy for the shunt-active filter.

Fig. 20 shows voltage waveforms on the 154-kV bus and the voltage imbalance factor before and after compensation, measured at 14:20–14:30 on July 27, 1994. The active filters are effective not only in compensating for the voltage impact drop and variation, but also in reducing the voltage imbalance factor from 3.6% to 1%. Here, the voltage imbalance factor is the ratio of the negative to positive-sequence component in

the three-phase voltages on the 154-kV bus. At present, several active filters in a range of 40–60 MVA have been installed in substations along the Tokaido Shinkansen [25].

X. Conclusion

This paper has presented a survey of the state-of-the-art of power electronics in Japan, with the main focus on technology relevant to medium–high-power applications. Power electronics technology has brought high performance, high efficiency, energy savings, high reliability, maintenance-free operation, and compactness to all electrical and electronic equipment. The author expects the continued efforts of power electronics researchers and engineers, including himself, to make more significant progress in power electronics technology by 2006 than that made in the last ten years.

Acknowledgment

The author would like to thank Prof. J. G. Kassakian of the Massachusetts Institute of Technology for his suggestions and English-language editing.

References

[1] T. Hasegawa, K. Yamaji, H. Irokawa, H. Shirahama, C. Tanaka, and K. Akabane, "Development of a thyristor valve for next generation 500 kV HVDC transmission systems," *IEEE Trans. Power Delivery*, vol. 11, no. 4, pp. 1783–1788, 1996.

[2] K. Imai, "Power electronics strives to be friendly to the environment," *IEEE Trans. Power Delivery*, vol. 11, no. 4, pp. 1783–1788, 1996.

[3] A. Nakagawa and Y. Seki, "Future trends in power semiconductor devices," in *Proc. 1996 IEE Japan Annu. Convention*, no. S.15-1 (in Japanese).

[4] Y. Takahashi, K. Yoshikawa, M. Soutome, T. Fujii, M. Ichijyou, and Y. Seki, "2.5 kV 1000 A power pack IGBT," in *Proc. 8th Int. Symp. Power Semiconductor Devices and ICs*, Maui, HI, 1996, pp. 299–302.

[5] H. Kobayashi *et al.*, "3.5 kV IGBT," in *Proc. 1996 IEE Japan Annu. Convention*, no. 752 (in Japanese).

[6] M. Honbu, "Present status of the development of high-power inverters," in *Proc. 1992 IEE Japan Annu. Convention*, no. S.8-3 (in Japanese).

[7] A. Nabae, I. Takahashi, and H. Akagi, "A new neutral-point-clamped PWM inverter," *IEEE Trans. Ind. Applicat.*, vol. 17, no. 5, pp. 518–523, 1981.

[8] H. Okayama, M. Kayo, S. Tammy, T. Fujii, R. Ached, S. Mizoguchi, H. Ogawa, and Y. Shimomura, "Large capacity high performance 3-level GTO inverter systems for steel main rolling mill drives," in *Proc. 1996 IEEE/IAS Annu. Meet.*, pp. 174–179.

[9] H. Takaoka and O. Tanaka, "Development of large capacity three-level IGBT inverter," in *Proc. 1996 IEE Japan Annu. Convention*, no. 794 (in Japanese).

[10] D. M. Divan, "The resonant dc link converter—A new concept in static conversion," in *Proc. 1986 IEEE/IAS Annu. Meet.*, pp. 648–656.

[11] M. Kaneda and Y. Sekino, "High-frequency power supply systems for tube welding," *Meiden Jiho*, vol. 248, no. 3, pp. 11–16, 1996 (in Japanese).

[12] H. Fujita and H. Akagi, "Pulse-density-modulated power control of a 4 kW 450 kHz voltage-source inverter for induction melting applications," *IEEE Trans. Ind. Applicat.*, vol. 32, no. 2, pp. 279–286, 1996.

[13] M. Hattori, "Future trends of power electronics in industry," in *Proc. 1996 IEE Japan Annu. Convention*, no. S.15-4 (in Japanese).

[14] T.-H. Chin, Y. Miyasita, and T. Koga, "Sensorless induction motor drives: An innovative component for advanced motion control," in *Proc. 1996 Int. Federation of Automatic Control*, San Francisco, CA, vol. A, pp. 445–450.

[15] H. Umida, "System configurations of speed-sensorless vector control," *Proc. Inst. Elect. Eng.*, vol. 117-D, no. 5, pp. 541–543, 1997 (in Japanese).

[16] Y. Miyasita, A. Imayanagida, and T. Koga, "Recent industrial application of speed-sensorless vector control in Japan," in *Proc. 1994 IEEE/IES IECON*, pp. 1573–1578.

[17] Y. Ohmori, T. Nakanishi, and H. Kobayashi, "A speed-sensorless spatial vector controlled inverter adding an auto-measuring function," in *Proc. 1995 European Power Electronics Conf.*, Seville, Spain, 1995, vol. 3, pp. 452–457.

[18] S. Kitamura *et al.*, "HVDC system technologies," *Toshiba Rev.*, vol. 49, no. 6, pp. 1–28, 1994 (in Japanese).

[19] E. Kita, M. Nishi, K. Saito, and A. Bando, "A 400 MW adjustable speed pumped-storage system," *Water Power Dam Construction*, pp. 37–39, 1991.

[20] S. Mori, E. Kita, H. Kojima, T. Sanematsu, A. Shibuya, and A. Bando, "Commissioning of 400 MW adjustable speed pumped-storage system for Ohkawachi hydro power plant," in *Proc. 1995 Cigre Symp.*, 1995, no. 520-04.

[21] S. Furuya, F. Wada, K. Hachiya, and K. Kudo, "Large capacity GTO inverter-converter for double-fed adjustable speed system," in *Proc. 1995 Cigre Symp.*, 1995, no. 530-04.

[22] H. Akagi, "New trends in active filters for power conditioning," *IEEE Trans. Ind. Applicat.*, vol. 32, no. 6, pp. 1312–1322, 1996.

[23] A. Iizuka, M. Kishida, Y. Mochinaga, T. Uzuka, K. Hirakawa, F. Aoyama, and T. Masuyama, "Self-commutated static var generators at Shintakatsuki substation," in *Proc. 1995 Int. Power Electronics Conf.*, Yokohama, Japan, 1995, pp. 609–614.

[24] H. Akagi, Y. Kanazawa, and A. Nabae, "Instantaneous reactive power compensators comprising switching devices without energy storage components," *IEEE Trans. Ind. Applicat.*, vol. 20, no. 3, pp. 625–630, 1984.

[25] M. Takeda, S. Murakami, A. Iizuka, M. Hirakawa, M. Kishida, S. Hase, and H. Mochinaga, "Development of an SVG series for voltage control over three-phase unbalance caused by railway load," in *Proc. 1995 Int. Power Electronics Conf.*, Yokohama, Japan, 1995, pp. 603–608.

Hirofumi Akagi (M'87–SM'94–F'96), for a photograph and biography, see this issue, p. 322.